Conceptual Design of a 10-Mw_e Nuclear Rankine System for Space Power

JOHN H. PITTS* AND CARL E. WALTER†
Lawrence Radiation Laboratory, University of California, Livermore, Calif.

The conceptual design of a 10-Mw_e Rankine system for nuclear-electric space power is described. A compact nuclear reactor operating at 1650°K (~2500°F) uses uranium mononitride as the fuel, lithium as the coolant, and tungsten-25% rhenium as a structural material. The reactor is controlled by a dual control system consisting of lithium-6 liquid control tubes and a movable molybdenum side reflector. A lithium-hydride and tungsten nuclear shield, which reduces radiation to an acceptable dose for a manned payload over a 10,000-hr life, is provided. The shield accounts for about half the total system specific mass of 7 kg/kw_e. A lightweight heat-pipe radiator rejects waste heat at 1100°K (~1500°F). Over-all system efficiency is 17.5%.

Introduction

THE Lawrence Radiation Laboratory at Livermore (LRL) was engaged in a program to develop the technology for building advanced, high-temperature reactors for nuclear-electric space power systems. Reactor concepts were examined for application to liquid-metal Rankine cycle, out-of-pile thermionic, and other conversion systems that might be in operation sometime after 1980, in the power range from tens of kilowatts to several megawatts. This report presents a conceptual design of a 10-Mw_e, Rankine-cycle, nuclear-electric space power system, with an over-all system efficiency of 17.5%. Designated SPR-6, this design was partially optimized to obtain a low power plant specific mass combined with high system reliability. Its primary application would be to provide propulsion energy for manned, interplanetary missions such as manned Mars-landing missions.[1] Its design point of 10-Mw_e for 10,000 hr was chosen to correspond to such expeditions. However, the reactor performance and design are adaptable to a wide variety of space missions.

General System Description

The SPR-6 power plant pictured in Fig. 1 depicts the 57-Mw reactor, nuclear shield, and power conversion equipment. A schematic diagram of the SPR-6 system showing various state points is presented in Fig. 2. (Primary design emphasis was placed on the reactor, nuclear shield, and heat-pipe radiators.) High-purity liquid lithium is heated in a reactor and pumped through a heat exchanger, which boils the potassium working fluid. Each of four turbine-alternator units extracts 2.5-Mw_e of useful power from the working fluid. Waste heat is rejected through an efficient heat-pipe radiator. The reactor is separated from all the other components by the main lithium hydride (LiH) shadow shield, which effectively blocks any direct radiation between materials on the reactor side and the components as well as the manned payload on the other side. The payload dose plane was taken to be 10 m diam located 50 m from the reactor.

Reactor control for operational shutdown, temperature effects, and lifetime effects ($\Delta k = 0.048$ total) may be obtained from either in-core liquid control circuits or by axial translation of the side reflector. Once a nearly neutral coolant mixture has been achieved in the reactor loop, each system is capable of independently controlling the reactor.

The boiler contains tantalum tubes arranged in a triangular pattern and separated from each other to allow the liquid lithium coolant to circulate around the tubes. Pressure in the reactor loop is adjusted to minimize the pressure difference across the boiler tube walls. The boiler is positioned on the payload side of the shield to reduce the activation of the natural potassium working fluid to acceptable levels.

A flat, rectangular heat-pipe radiator is used to reduce the mass of the main radiator to about one-half that of a conventional fin-and-tube type. The heat pipes operate in parallel and thus offer the advantage of redundancy. The flow rate through the heat-pipe radiator loops is varied by adjusting the power to three mechanical pumps. Additional redundant pumps can be introduced with only a small mass penalty. A liquid-metal storage-expansion tank is required in each loop to maintain the desired system pressures.

A mass breakdown is given in Table 1. The low specific mass (α) of 7 kg/kw_e is made possible by postulating a high fuel burnup capability, high-strength alloys, a compact radiation shield, and highly efficient heat-pipe radiators. The smallest reasonable reactor is utilized, since reactor size

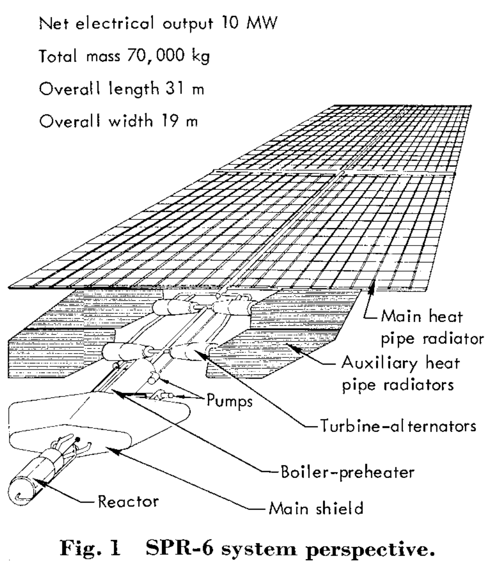

Fig. 1 SPR-6 system perspective.

Received August 4, 1969; revision received December 22, 1969. This work was performed under the auspices of the U.S. Atomic Energy Commission. We are indebted to the former Nuclear Space Power Staff at the Lawrence Radiation Laboratory, Livermore, for their support and contributions.

* Mechanical Engineer.
† Mechanical Engineer. Member AIAA.

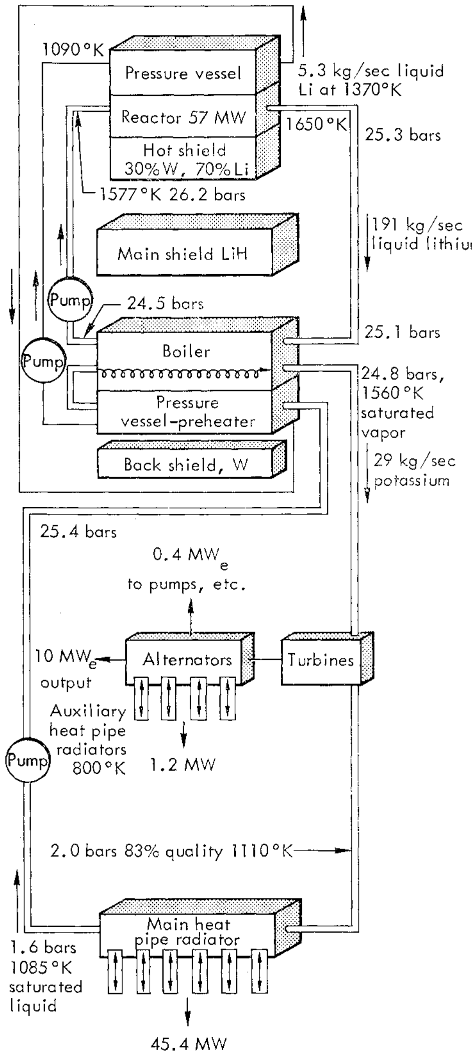

Fig. 2 SPR-6 system schematic.

affects not only the mass of the reactor but that of the shields as well. This low specific mass is a desirable attribute regardless of application but is particularly important to electric propulsion missions.[1]

Interactions between the reactor and other parts of the system were examined by combining performance characteristics of each component into a single system model and varying the important thermodynamic parameters one at a time. Minimum system mass was selected as an optimum parameter, but because of the changing nature of the system model and assumptions made during the optimization studies, the SPR-6 system described is only partially optimized.

The optimum reactor outlet temperature T_{ro} is $\sim$1650°K. For lower T_{ro}'s, a larger and heavier radiator is required to reject waste heat. At higher T_{ro}'s the piping and containment vessel masses increase and the turbine blades are overstressed. A turbine temperature ratio (T_{to}/T_{ti}) of 0.7 was found to give a minimum α for the system. Because of the large size, the power plant would be launched in a partially assembled condition and some manual work would be required in low earth orbit to ready the system for operation.

SPR-6 Reactor

General Description

The design of the SPR-6 reactor is based on uranium mononitride (UN) as the fuel, lithium as the coolant, with an alloy of 75% tungsten and 25 % rhenium as the structure. Compatibility of these materials at operating temperatures is substantiated by experimental data.[2]

Figure 3 is an isometric drawing of the SPR-6 reactor; general characteristics are given in Table 2. The core of the reactor is composed of a close-packed bundle of 8000 fuel elements and half that many coolant channels supported on the downstream end by a 30-cm-thick tungsten structure and on the upstream end by a spline attachment, to provide for axial and radial growth. The downstream support structure also acts as a radiation shield.

In cross section, the active core is an annular region surrounding a central coolant-return passage and a liquid control region. The outer boundary of the core is a dodecagon to accommodate the hexagonal packing pattern of the fuel elements. The fueled core is enclosed by thin, polygonal, W-25% Re membranes at the inner and outer radii.

A slight radially inward net pressure is produced on the outer membrane by venting stagnant lithium fluid present between the core and the pressure vessel to the upstream pressure. A slight radially outward net pressure exists across the inner membrane because of the core pressure drop. Thus, the core acts as a rigid column between the upstream and downstream supports, dynamically restrained by the side membranes and the radial pressure gradients. This concept of a dynamically restrained core prevents changes in position of the fuel elements and keeps the flow passages aligned.

A 1.2-cm-thick, cooled, tantalum pressure vessel and a segmented 2-cm-thick molybdenum side reflector surround the core (Fig. 3). The reactor pressure vessel is clad on the inner surface with tungsten, so that the reactor coolant is exposed only to the UN fuel and tungsten base materials. A separate cooling loop keeps the reactor pressure vessel, as well as the boiler-preheater pressure vessel, at temperatures below 1400°K. Although this cooling loop adds some complexity to the system, it minimizes the reactor-vessel thickness, which in turn enhances the side reflector control worth, reduces the over all system mass, and simplifies the fabrication of the pressure vessel. It extracts heat from the reactor and boiler-preheater pressure vessels by conduction and transfers it to potassium liquid in the preheater.

The reactor coolant is returned to the reactor by a 15.3-cm-diam central duct. An annular region 3.7-cm-thick surrounding the central duct contains liquid lithium control circuits. Pressure drop in the reactor coolant return duct is about 10% of that in the core. The optimum cross-sectional area of the reactor coolant return duct plus the annular control region is about 15% of the fueled core area.

The radial power profile is flattened by varying the U^{235} enrichment in four annular zones. Radial peak-to-average power density ratio is 1.12. Axial U^{235} enrichment is uni-

Table 1 Mass breakdown for 10 Mw$_e$ SPR-6 system

	100 kg	%
Shields	330	47.2
Main radiator	134	19.1
Alternators (including auxiliary cooling radiators)	72	10.2
Reactor	42	6.1
Boiler-preheater	18	2.6
Structure	15	2.1
Turbines	14	2.0
Reactor loop piping	10	1.4
Lithium coolant pump	10	1.4
Potassium working fluid pump	6	0.9
Lithium fluid	6	0.9
Power conversion loop piping	5	0.7
Potassium fluid	4	0.6
Controls	3	0.4
Pressure vessel cooling loop pump	1	0.1
Miscellaneous	30	4.2
Total, 100 kg	700	100.0 %

form and yields the usual cosine-power density distribution with a peak-to-average value of 1.4.

Materials Selection

The selection of UN, Li, and W-25% Re, for the reactor was based on both neutronic and chemical considerations. For the fuel, UN combines several favorable characteristics: high uranium density, good thermal conductivity, high melting point, satisfactory nuclear properties, relatively good properties for fabrication and handling, and a relatively low tendency to swell with burnup. The nitrogen present in the fuel has low affinity both for lithium and for W-Re alloys. The nitride was chosen over the sulfide, because more information was available and because nitrides add potential strength to the tungsten alloys being considered. The oxide was rejected because it would react strongly with the lithium coolant, should the cladding fail. The carbide is reactive unless the stoichiometry (U/C ratio) is precisely controlled, which is difficult.

A potential danger exists in the use of UN at high temperatures, where there is a tendency to lose the nitrogen, which would release free uranium with a high chemical activity. It may be necessary to operate the reactor with an overpressure of N_2 to suppress this tendency, so that the fuel elements would operate within the one-phase region shown in Fig. 4. A nitrogen overpressure of 10^{-4} torr was chosen for the SPR-6 design temperature of 1650°K. At temperatures below about 1570°K, the nitrogen overpressure is probably not necessary.

Lithium was chosen as the reactor loop coolant in preference to other liquid metals because of its low corrosive

Table 2 Characteristics of SPR-6 reactor

Average fuel atom burnup, %	2.1
Maximum fuel atom burnup, %	3.3
Average fuel enrichment, atom fraction of U^{235}	0.70
Maximum fuel enrichment, atom fraction of U^{235}	1.0
Average fuel power density, w/cm^3	575
Radial peak-to-average power density	1.12
Overall peak-to-average power density	1.57
Average neutron energy, Mev	0.25
Prompt neutron lifetime, l^*, nsec	81
Fueled core length, cm	87.0
Fueled core mean outer diameter, cm	62.1
Liquid-lithium control zone outer diameter, cm	22.7
Reactor coolant return duct diameter, cm	15.3
Pressure vessel inside diameter, cm	65.0
Side reflector inside diameter, cm	67.4
Side reflector outside diameter, cm	71.4
Fuel radius, cm	0.216
Fuel element cladding inside radius, cm	0.225
Fuel element cladding outside radius, cm	0.250
Coolant tube inside radius, cm	0.220
Number of fuel tubes	8064
Number of coolant tubes	4032
Fuel volume fraction	0.433
Cladding, plus coolant tube volume fraction	0.183
Primary coolant volume fraction	0.234
Interstitial fluid volume fraction	0.093
Swelling allowance volume fraction	0.057
Total fueled core volume, m^3	0.228
Reactor coolant flow rate, kg/sec	191
Reactor coolant outlet temperature, °K	1650
Reactor coolant temperature rise, °K	73
Reactor coolant inlet pressure, bars	26.2
Reactor pressure drop, bars	0.9
Core Reynolds number	5.9×10^4
Reactor coolant velocity inside core, cm/sec	740
Average heat flux at coolant channel surface w/cm^2	117
Average centerline fuel temperature, °K above local coolant temperature	46

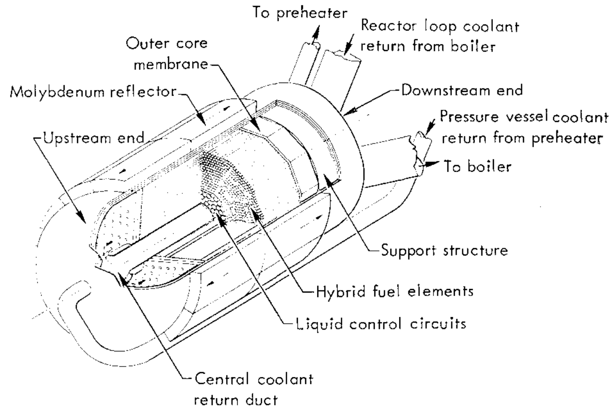

Fig. 3 SPR-6 reactor isometric drawing.

effect on refractory metals, low activation cross section, low vapor pressure, and good heat-transfer properties. The nuclear properties of Li^6 and Li^7 are particularly advantageous since the amount of the strong neutron absorber, Li^6, mixed in the reactor coolant can be utilized for adjustments of the reactivity and control of the reactor. The relatively low vapor pressure of lithium minimizes the possibility of boiling inside the reactor, and gives lower stress in the reactor piping.

The cladding must resist dissolution by the hot flowing coolant and must not react adversely while in intimate contact with the fuel. The structure, in addition, should provide maximum resistance to deformation at high temperatures. Of all the metals, tungsten offers the greatest potential for the cladding and structure and is the outstanding candidate for the ultimate reactor. Semitheoretical considerations predict that tungsten has a creep rate far lower than Ta or Mo at SPR-6 temperatures, and that its solubility in molten Li is extremely low. It is chemically compatible with UN because of the thermodynamic instability of tungsten nitride. Unfortunately, pure tungsten cannot be fabricated into the shapes required for the reactor, and it is prohibitively brittle at room temperature. For this reason, W-25% Re was selected for the reactor cladding and structure, especially since it has appreciable room-temperature ductility and can be fabricated by relatively conventional techniques.

Reactor Design

Numerical specifications of the reactor were determined with a modified version of the one-dimensional neutron transport code, DTF,[3] with an S_4 approximation, This DTF

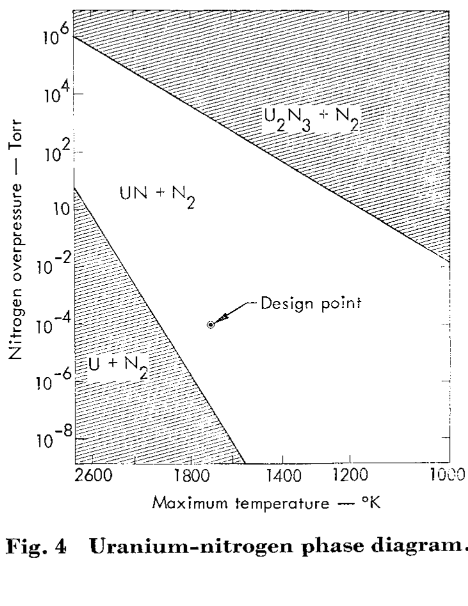

Fig. 4 Uranium-nitrogen phase diagram.

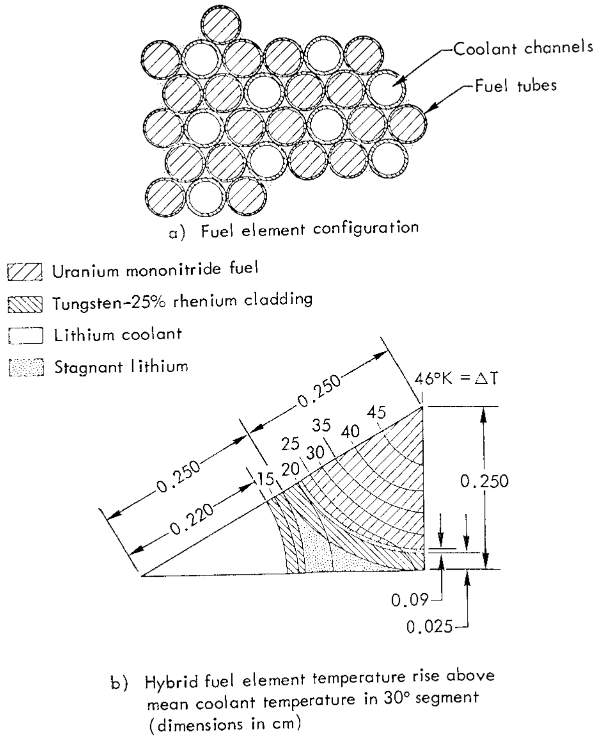

Fig. 5 SPR-6 hybrid fuel element.

code was coupled to a thermodynamic program which permitted use of a variety of thermomechanical constraints.

The core contains hybrid-type fuel elements in an arrangement of close-packed, equal-diameter metal tubes (see Fig. 5). Every third tube is unfueled and serves as a reactor coolant passage. Interstices between the tubes are filled with stagnant liquid Li. The temperature distribution of the hybrid elements, shown in Fig. 5, does not vary significantly from that of a uniformly cooled rod, due to the high and nearly equal value of the thermal conductivities of lithium and tungsten. Allowance for fuel swelling due to burnup is provided by a small gap between the fuel pellets and the cladding. This hybrid fuel element has several advantages. Cladding redundancy exists, since the flowing Li is separated from the fuel by a double wall. Fuel swelling is permitted without dimensional changes in the fuel tube cladding. This adds structural stability to the core and decreases temperature effects on reactivity. Element assembly is simple and has apparent reliability. Although the low fuel volume fraction results from the use of hybrid fuel elements, reactor criticality is easily achieved.

Linear swelling in the fuel is assumed to be equal to twice the burnup fraction. An average 2% burnup limit appears to be reasonable in light of available material data. There is little difficulty accommodating fuel swelling up to twice that assumed. The swelling-allowance gap is initially filled with liquid lithium bonding fluid. Nominal circulation of this fluid permits continuous separation of fission products. Acceptable fuel element dimensions can vary over a wide range.

Nuclear ground safety prior to reactor operation is provided by initially filling the fueled core with lithium having 28% enrichment in the neutron-absorbing isotope Li^6, and by filling the remaining volume of the reactor coolant loop with Li^7. The increased concentration of Li^6 in the fueled core during ground handling renders the reactor subcritical by 10% Δk. This isotope separation is easily maintained since lithium is solid below 450°K.

At the beginning of reactor life, the Li throughout the reactor coolant loop is melted. Subsequently it is circulated until a homogeneous mixture of 97% Li^7 and 3% Li^6 is formed in the reactor coolant loop. This, in effect, removes Li^6 from the fueled core and renders the reactor near critical. The advantage of this ground safety concept lies in the absence of mechanical devices in the reactor.

The low melting temperature of Li (450°K) and the compact arrangement of the reactor coolant loop permit melting to be accomplished readily by external heaters.

Redundancy in reactor control is assured through two independent control systems—a mechanical side reflector and a liquid control system. This dual-control system exhibits several advantages over a single-control scheme. The required adjustable reactivity range of each control system can be held relatively small, since reactivity reserves and provisions for failure of individual segments of each system are accounted for by the backup controls. Either system, by itself, could carry the mission to completion. In the mechanical control system, variations in reactivity are made by axially translating segments of the 2-cm-thick molybdenum side reflector. In the liquid control system, lithium control tubes are positioned in a 3.7-cm-thick annulus between the central duct and the fuel core. These tubes can either be filled with or voided of Li^6, which acts as the neutron-absorbing medium. They are double-walled as an added precaution to prevent accidental transfer of Li^6 into the main coolant stream, and they contain metal screens in the form of capillary wicks, similar to those in heat pipes, to allow uniform distribution of the liquid Li under zero-gravity conditions.

Since the mechanical and the liquid control systems act respectively on the periphery and inner boundary of the fueled core, there is little interdependence between the systems. This is brought out clearly by Fig. 6, which shows the control range of the dual-control system. A particular reactivity state can be achieved with several combinations of the individual controls, as long as their combined effect matches that of the desired reactivity requirement. This is illustrated in Fig. 6 by the shaded area for achievement of criticality at the beginning of life with the reactor at 600°K. The solid arrow indicates a possible path.

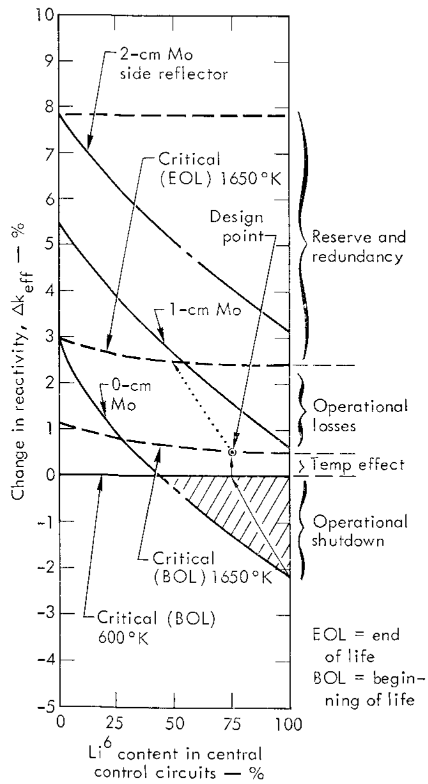

Fig. 6 SPR-6 dual-control system reactivity range.

The design point for the dual-control system was chosen with 75% Li^6 in the control system and an equivalent 0.7-cm-thick side reflector. This renders the reactor critical at the beginning of life and at the design temperature of 1650°K.

Nuclear Shield

The reactor shielding was designed to reduce the total integrated dose to the crew to 13.3 rem. This value was set by utilizing a maximum of 100 rem for Baum's "effective residual dose"[4] partitioned as shown in Table 3. With a constant dose rate, 3 rem of effective residual dose is given by a real dose of 13.3 rem.

Shield calculations were performed with GEISHA computer code using point kernel methods.[5] Removal theory, with Albert-Welton[6] fit to experimental data for hydrogenous materials, was employed for neutrons. Six energy groups and appropriate buildup factors were used for gamma ray calculations. Secondary gamma-ray production was accounted for by assuming that all the fast neutrons "removed" within a component are absorbed within that same component.

A three-part shield configuration was assumed in the calculations. The first component, called the "hot shield," is a region 30-cm long located within the reactor vessel. This region includes the reactor downstream support structure and is considered to have a volumetric composition of 70% Li and 30% W. Since reactor-loop Li coolant flows through this hot shield region, any heat deposited here is easily removed.

The next component, the main shield, formed of LiH, is positioned so that its maximum temperature would be 800°K or less. For an integrated dose of 13.3 rem at the payload center, the required thickness was determined to be 113 cm, but, to account for the effects of the necessary shield penetrations, a 140-cm-thick main shield is used. Lastly, the back shield, a 12-cm-thick slab of tungsten, shields the payload from 1) secondary γ rays produced in the hot and main shields, 2) scattered γ rays, and 3) bremsstrahlung produced in the piping and boiler. The third source results from the activation of the Li^7 in the coolant (reaction is $Li^7 + n \rightarrow Li^8 \xrightarrow{0.85\ \mathrm{sec}} 2\alpha + \beta^-$). The resulting beta particles produce γ rays with energies from zero to 13 Mev by the bremsstrahlung process.

To prevent scattered radiation from reaching the payload, "wings," extensions of the main LiH shield, were designed to cast a shadow over the components on the payload side of the shield. Approximate scattering calculations indicated that a wing thickness equal to the central portion of the main shield would provide more than the required attenuation for neutrons. The tungsten back shield is extended around the boiler and along the wings to similarly reduce the dose from scattered γ rays.

Figure 7 displays the results of a parameter study, using varied hot and back shield thicknesses. The normalized mass of the complete shield is indicated as a function of the thickness of its components. A broad minimum exists at about 30 cm of hot shield and 12 cm of back shield. While the total mass varies little over this range, the shield design varies considerably.

Table 3 Contributions to the payload effective residual dose

	Effective residual dose, rem
Trapped radiation (Van Allen belt)	5
Galactic radiation	3
Power plant maintenance	25
Reactor operation	3
Solar flares	64
Total	100

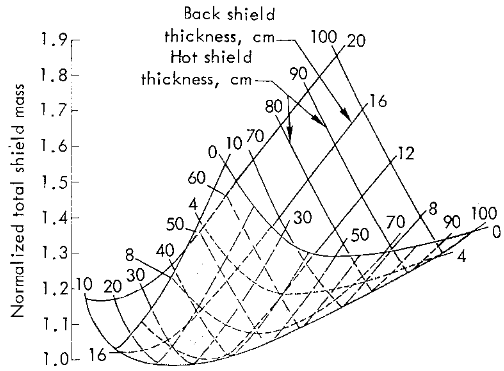

Fig. 7 The effect of hot shield and back shield thickness on normalized total shield mass for a given integrated payload dose of 13.3 rem and a maximum main shield temperature of 800°K.

Power Conversion

Heat Pipe Radiators

Lightweight power plants require a reliable method of rejecting waste heat that has low specific mass. The radiator studies conducted at LRL started with classical fin-and-tube approach.[7,8] When optimum fin-and-tube radiators were found to be too heavy due to the required meteoroid protection, a change was made to a heat-pipe radiator. The heat-pipe approach, at SPR-6 power levels, proved to be a good choice, with a near-optimum design specific mass of 1.34 kg/kw$_e$.

The heat-pipe radiator differs in design principle from a vapor fin radiator (which also employs heat pipes) in two important respects: a) direct contact between the heat pipes and the fluid to be cooled (see Fig. 8) considerably increases heat-transfer effectiveness, and b) the designer can freely select the relative proportions of heat-pipe area used for absorption and for dissipation of heat.

The main heat-pipe radiator is constructed of a series of manifolds, positioned in a rectangular array, whose walls are penetrated by a large number of heat pipes. The manifolds and other ducting carry the same amount of meteoroid protection as required in other radiator designs. However, because their presented area is small, they do not contribute greatly to the total radiator mass. The heat pipes transfer heat at a substantially isothermal condition, operate in parallel, and are functionally independent of each other. Minimum radiator mass occurs when they are designed so that some will fail during lifetime due to meteoroid penetration. An excess of heat pipes is installed at the beginning of life, and the pipe wall thickness is determined so that approximately 10% of the heat pipes fail from meteoroid penetration during their lifetime. A punctured heat pipe will cool at its outer end and will not contribute significantly to the heat exchange.

The main heat-pipe radiator characteristics are shown in Table 4. Niobium is used for the structural tube material

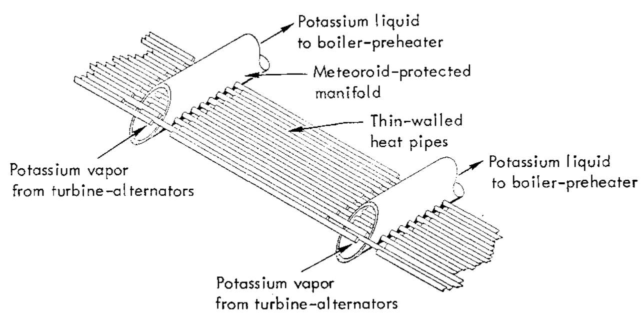

Fig. 8 Main radiator heat-pipe layout.

Table 4 Heat-pipe radiator characteristics

	Main radiator	Auxiliary radiators
Total heat rejection required, kw	45.4	0.3 per radiator
Total projected area (including piping and manifolds), m^2	400	10 per radiator
Total radiator mass, kg	13,400	300 per radiator
Number of heat pipes	24,000	100 per radiator
Number of radiators	1	4
Heat pipe fluid	Potassium	Sodium
Heat pipe rejection temperature, °K	1080	800
Heat pipe radial input flux, w/cm^2	50	50
Heat pipe inside diameter, cm	1.5	2.4 to 3.0 (in radiator) 1.7 (in alternator area)
Radiator survival probability	0.99	0.99

with beryllium for a meteoroid barrier where required. A radiator over-all survival probability of 0.99 was used to determine the thickness of the meteoroid barrier.

The effects of various parameters on the SPR-6 main radiator mass were investigated. While the parameter variation was not exhaustive, it was enough to specify a near-optimum main heat-pipe radiator design. The radiator survival probability was found to be the major parameter affecting the radiator mass. The radiator mass penalty incurred to increase the survival probability from 0.99 to 0.999 is less than 50%.

Auxiliary heat-pipe radiators to cool the alternator windings were similar in design to the main radiator, except that the heat pipes were inserted directly into the area around the windings. Heat from the windings is removed by conduction to heat pipes that utilize sodium as a working fluid. The auxiliary radiator rejection temperature is 800°K as shown in Table 4.

Turbine-Alternators

Although the turbine-alternators account for only one-sixth the total system mass, their efficient performance has a direct influence on the size of most other components and therefore on the system mass. Consequently, a brief investigation was conducted to determine the general effects on performance of specified parameters such as working fluid, number of units, and rotational speed.

The turbines selected are the full-admission axial flow type with 20–40% reaction per stage. Each turbine has seven stages and an over-all efficiency of 78%. To simplify the analysis, moisture removal and interstage drainage (which might be necessary because of turbine erosion problems) were not included. Instead, a performance penalty of $\frac{1}{2}$% efficiency for each 1% of exit moisture was assumed throughout the turbine analysis.

The selection of potassium as the working fluid in the power conversion loop was based on turbine efficiency and size, over all system mass, and available data on operating liquid metal turbines. Primarily, sodium, potassium, and cesium were considered. Sodium turbines tend to be larger in size and to contain more stages than potassium turbines operating under the same conditions. Cesium turbines are smaller and more efficient, but cesium's high vapor pressure requires larger masses for other components and results in a higher over-all system mass.

The selection of four turbine-alternator units to generate a combined 10-Mw_e output was based on reliability considerations. A smaller number of units would result in an excessive reduction of total output power should one of the units malfunction. On the other hand, more units would add additional complexity to the system.

Table 5 Assumed mechanical pump operating characteristics

Pump efficiency	0.50
Motor efficiency	0.75
Cycloconverter efficiency	0.90
Transformer efficiency	0.98
Power factor	0.85

Rotational speed is limited by the maximum allowable stress in the turbine blades and alternator rotors. A rotational speed of 12,000 rpm was selected since it was compatible with standard alternator frequencies and since turbine-alternator mass varies inversely with rotational speed. Several typical, high-temperature turbine blading materials were considered, among them the molybdenum alloys of TZM and TZC as well as the tungsten alloy designated "Sylvania A." Allowable blading stress was set at the value resulting in a 1% creep in 10,000 hr. The material selected as representative for the SPR-6 turbines was TZC. Allowable stress values were based on the use of molybdenum alloys for the turbine structural members and H-11 steel with a nickel alloy core for the alternator rotors.

The SPR-6 alternator is a radial-gap homopolar machine with a single field coil, located on the stator. This type of unit features a solid forged-steel rotor with a nickel alloy core that requires no rotating windings, slip rings, or rectifiers.

Both stator and field coil windings are cooled by sodium heat pipes imbedded in the outer edge of the stator. These pipes extend in a planar array to form radiators and operate at 800°K. Energy is transmitted from the stator teeth and electrical conductors to the heat pipes by thermal conduction. Thermal conduction out of the field coil region is facilitated by copper sheets imbedded in the windings. Over-all alternator efficiency was 90%.

Dynamic seals are provided at each end of the rotor to keep the generator cavity pressure at about 0.1 torr. This pressure level was selected to permit thermal coupling between various components of the alternator and because fluid friction losses are minimized by assuring vaporization of any potassium in the cavity. The alternators each utilize two potassium-lubricated bearings and are directly coupled to the turbines.

The electromagnetic analysis used for design of the alternators was based on a method of Jain.[9] This method was used to establish optimum values of stator current density, current loading, and pole pitch. These optimum values were used in a new set of calculations to determine the best choice of frequency. A value of 2400 Hz was found to give a minimum alternator specific mass. A voltage of 2400 v was selected to be reasonable from a standpoint of insulation breakdown in the alternator and to aid in reducing thruster power-conditioning mass.

Boiler-Preheater

The boiler-preheater is constructed in the counter-flow, shell-and-tube arrangement. Subcooled potassium from the radiator first enters a preheater section consisting of an annular region that surrounds the main boiler tube array. Heat transferred from the cooling-loop liquid lithium to the subcooled potassium in this preheater section permits both the reactor and boiler vessels to be cooled below 1400°K. The potassium, still subcooled, enters the 2900 (approximate) boiler tubes (each 1 cm in diam and 154 cm long) and leaves as saturated vapor. A helical flow swirler is positioned inside each boiler tube to keep the liquid portion of the potassium next to the tube wall and prevent boiling instability. The boiler tubes are separated slightly from each other to permit adequate flow of the reactor loop coolant around the outside surfaces of the tubes.

Reactor-loop liquid lithium coolant enters the boiler at 1650°K, flows around the boiler tubes in a single-pass, cross-counterflow arrangement, and exits at a temperature of 1577°K. Fluid in the pressure vessel cooling-loop flows in the annular preheater area in a single-pass counterflow direction. The tantalum-alloy boiler vessel wall is cooled by the cooling-loop fluid, which in turn is cooled by the power-conversion loop potassium.

The boiler tubes are constructed of a 0.025-cm thick, tantalum alloy, clad with tungsten on the outside surface. This tube wall thickness was selected as being practical from a manufacturing standpoint. Problems of structural integrity and leak tightness are minimized by maintaining the fluids on both sides of the boiler tubes at approximately 25 bars (the saturation pressure for potassium at 1560°K). The liner separating the boiler and preheater sections is also clad with tungsten on the inside so that only tungsten metal is in contact with the reactor loop coolant.

Heat transfer in the boiler is dominated by the potassium heat-transfer coefficient in the large two-phase region inside the tubes. On the basis of experimental data,[10,11] a conservative value of 0.85 w/cm^2-°K was selected for an average boiler heat-transfer coefficient. In actuality, the boiler heat-transfer coefficient is a function of a number of parameters and varies along the length of the tubes. Calculations, simplified by taking this coefficient to be a constant, may be as accurate as more complicated schemes, where data are not available near the operating conditions picked for the boiler.

Pumps

Mechanical pumps were chosen for the SPR-6 system because they have higher efficiency and lower mass than electromagnetic pumps. Operating characteristics (Table 5) were estimated from other pumps used in the nuclear industry.[12] The power-conversion loop pump is actually a combination jet-mechanical type. The jet portion raises the inlet pressure to the mechanical portion sufficiently, so that cavitation is prevented. Variation in pump performance causes relatively minor effects on overall system operating characteristics and mass.

Conclusions

From this study, an advanced, high-power high-temperature nuclear-electric space power system appears to be feasible. The reactor design utilizes UN as a fuel, Li as a coolant, and W-25% Re as a structural material.

Hybrid fuel elements are selected for the reactor because they are easy to assemble and because they separate the fuel from the coolant with a double wall, thus increasing reliability. Fuel swelling is permitted without dimensional changes in the fuel tube cladding. Since fission gases are vented, high strength cladding material is not essential.

The radial power distribution in the reactor is improved by incorporating a central Li coolant return duct and the radially variable U^{235} enrichment in the fuel. A dual-control system, composed of a movable 2-cm-thick Mo side reflector and a number of central liquid-lithium control circuits, offers desirable redundancy. Each control system is independently capable of carrying the mission to completion.

Heat-pipe radiators reject waste heat from the system, thereby reducing the mass of the radiators to about one-half that of conventional fin-and-tube radiators. The planar radiator requires a winged conical shield, which provides adequate radiation protection for a manned payload.

The SPR-6 system with an operating potential of 10,000 hr is calculated to have a total system specific mass of 7 kg/kw_e and an over all efficiency of 17.5%.

References

[1] MacKay, J. S. et al., "Manned Mars Landing Missions Using Electric Propulsion," TN-D-3194, 1966, NASA.

[2] *Quarterly Report Advanced Space Nuclear Power Program, July through September 1967*, Pt. II, UCRL-50004-67-3, Lawrence Radiation Lab., Livermore, Calif.

[3] Carlson, B. G. et al., "DTF Users Manual, Vols. I–II," United Nuclear Corp., White Plains, N. Y., Report UNC Phys/Math 3321, 1963.

[4] Baum, S. J. "Recommended Ionizing Radiation Exposures for Early Exploratory Space Missions," *Aerospace Medicine*, Vol. 33, Oct. 1962, pp. 1182–1186.

[5] Wilcox, T., "GEISHA-II, A CDC-6600 Code for Use in Parametric Shielding Surveys," UCIR-151, Sept. 1966, Lawrence Radiation Lab., Livermore, Calif.,

[6] Albert, R. D. and Welton, T. A., "A Simplified Theory of Neutron Attenuation and its Application to Reactor Shield Design," WAPD-15 (Del.), Nov. 1950, Westinghouse Atomic Power Div., Pittsburgh, Pa.

[7] Werner, R. W. and Carlson, G. A., "Heat Pipe Radiator for a 50 MW_t Space Power Plant," UCRL-50294, June 1967, Lawrence Radiation Lab., Livermore, Calif.

[8] Haller, H., Lieblein, S., and Lindow, B., "Analysis and Evaluation of a Vapor Chamber Fin-Tube Radiator for High Power Rankine Cycles," TN-D-2836, May 1965, NASA.

[9] Jain, G. C., "Design Aspects of a Homoplar Inductor-Alternator," *IEEE Transactions on Power Apparatus and Systems*, Vol. 83, Oct. 1964, pp. 1009–1015.

[10] "Alkali Metals Boiling and Condensing Investigations," *Quarterly Progress Reports 9–12*, edited by G. L. Converse, and F. E. Tippets, NASA 3-2528, July 1967–July 1968, General Electric Co., Cincinnati, Ohio.

[11] Peterson, J. R., "High Performance 'Once-Through' Boiling of Potassium in Single Tubes," NASA 3-2528, Topical Rept., 1966, General Electric Co., Cincinnati, Ohio.

[12] Kelly, R. W., Wood, G. M., and Harman, H. V., "Development of a High Temperature Liquid Metal Turbopump," *Transactions of the ASME, Ser. A: Journal of Engineering for Power*, Vol. 85, April 1963, pp. 99–107.